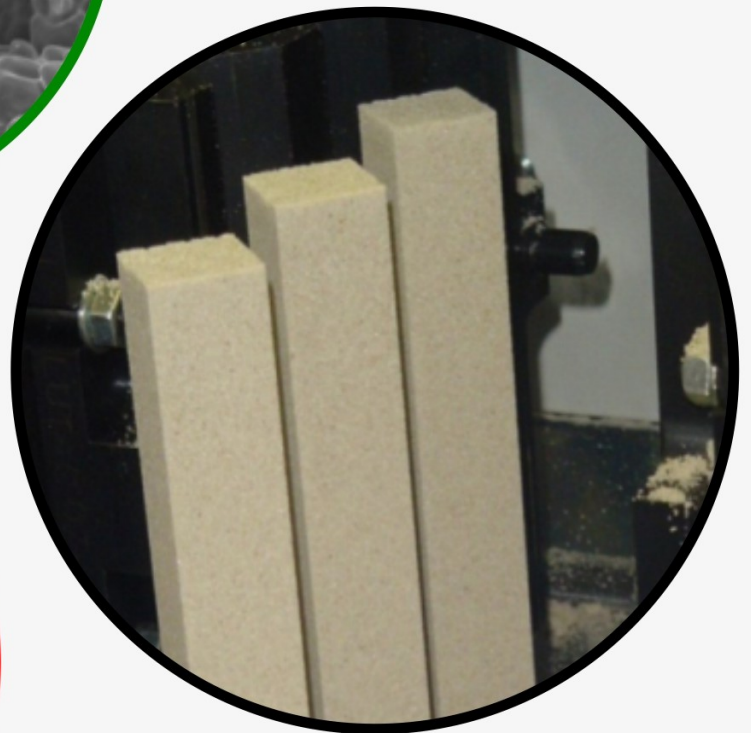
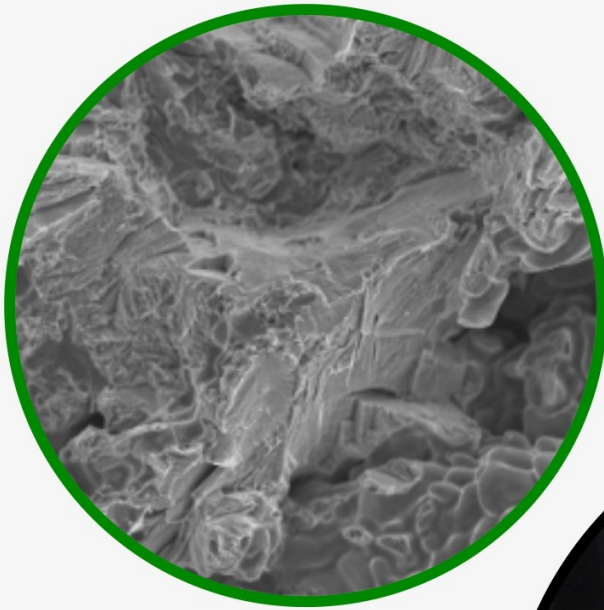


JOURNAL OF CASTING & MATERIALS ENGINEERING

QUARTERLY
Vol. 1 No. 3 / 2017

AGH UNIVERSITY OF SCIENCE AND TECHNOLOGY
FACULTY OF FOUNDRY ENGINEERING



JCME

Editor-in-Chief of AGH University of Science and Technology Press
Jan Sas

Editorial Board of *Journal of Casting & Materials Engineering*:

Editor-in-Chief

Beata Grabowska, AGH University of Science and Technology, Poland

Vice-Editor in Chief

Marcin Górny, AGH University of Science and Technology, Poland

Associate Editor

Franco Bonollo, University of Padova, Italy

Co-editors

Marcin Brzeziński, AGH University of Science and Technology, Poland

Jarosław Jakubski, AGH University of Science and Technology, Poland

Artur Bobrowski, AGH University of Science and Technology, Poland

Karolina Kaczmarek, AGH University of Science and Technology, Poland

Language Editor

Bret Spainhour

Technical Editor

Agnieszka Rusinek

Cover Designer

Małgorzata Biel

The articles published in the Journal of Casting & Materials Engineering have been given a favorable opinion by the reviewers designated by the Editorial Board.

www:

<https://journals.agh.edu.pl/jcme/>

© Wydawnictwa AGH, Krakow 2017



AGH UNIVERSITY OF SCIENCE AND TECHNOLOGY PRESS KRAKOW 2017

Wydawnictwa AGH (AGH University of Science and Technology Press)

al. A. Mickiewicza 30, 30-059 Kraków

tel. 12 617 32 28, 12 638 40 38

e-mail: redakcja@wydawnictwoagh.pl

<http://www.wydawnictwa.agh.edu.pl>

Contents

Bartosz Dęsoł, Renata Zapała, Paweł Pałka

Influence of Internal Scrap on Mechanical
Properties of Selected Cobalt Alloys

59

Mateusz Stachowicz, Patrycja Paduchowicz, Kazimierz Granat

Impact of Density Degree and Grade of Inorganic Binder
on Behavior of Molding Sand at High Temperature

64

Rafał Dańko, Łukasz Jamrozowicz

Density Distribution and Resin Migration Investigations
in Samples of Sand Core Made by Blowing Method

70

Influence of Internal Scrap on Mechanical Properties of Selected Cobalt Alloys

Bartosz Dęsoł^a, Renata Zapala^{a*}, Paweł Pałka^b

^a AGH University of Science and Technology, Faculty of Foundry Engineering, Reymonta 23, 30-059 Krakow, Poland

^b AGH University of Science and Technology, Faculty of Non-Ferrous Metals, Mickiewicza 30, 30-059 Krakow, Poland

*e-mail: zapala@agh.edu.pl

Received: 2 June 2017/Accepted: 18 September 2017/Published online: 9 November 2017

This article is published with open access at AGH University of Science and Technology

Abstract

This paper presents the results of mechanical tests carried out on two different commercially available cobalt alloys applied in dental prosthetics for the production of frame dentures. The test samples were obtained by the method of investment casting using as a charge pure primary materials and pure primary materials mixed with various additions of process scrap (25, 50, and 75%). The tests showed that the alloys could not reach the mechanical properties reported by the manufacturer in either case. In the case of the alloy without the addition of tantalum, the general conclusion was that both the plastic and strength properties decreased with increasing amounts of the introduced process scrap. The mechanical properties (mainly elongation) of the alloy containing Ta reached the highest values in the samples containing 75% of the process scrap. Examinations of fractures carried out by SEM have revealed their varied character – ductile or transcrystalline. All of the samples tested showed the presence of dendrites and solidification areas, with shrinkage porosity occurring in the internal sample zones.

Keywords:

cobalt alloy, mechanical properties, fracture, scrap

1. INTRODUCTION

Along with titanium alloys, nickel alloys and Cr-Ni steels, cobalt alloys belong to the group of common metal alloys that are widely used in medicine. Almost a century ago, the United States introduced the first cobalt alloy with chromium and molybdenum to dental surgery. The minimum chromium and molybdenum content in the alloy was 25% and 4%, respectively [1]. Contemporary cobalt alloys for biomedical applications are modifications of that alloy. In the as-cast state, the structure of cobalt alloys is comprised of the solid solution of chromium, molybdenum, and carbon in cobalt (and additionally, carbide precipitates) [2]. Occasionally, the CoCr phase may also appear in the alloy structure [3].

Cobalt alloys are characterized by satisfactory mechanical properties (e.g., elastic modulus); due to this fact, it is possible to manufacture products with thin walls and, as a consequence, lower weight [4]. The beneficial combination of high mechanical properties and relatively low manufacturing costs has opened a wide range of applications for cobalt alloys in dentistry, mainly for frame dentures, braces, and prostheses on latches, bolts, and locks [3].

Due to the intricate shape of these castings (including the numerous design modifications introduced to satisfy the individual biological needs of each patient and, additionally, the tendency of cobalt alloys to undergo the strengthening process during production), the implementation of

serial production is not possible. Products cast from these alloys are made by the investment technique. The use of investment casting in the manufacture of prosthetic parts generates large volumes of process scrap, including gating systems, casting cones, and rejects. Manufacturers allow the possibility to use scrap as part of the charge, but it should be remembered that any scrap metal introduced to the charge can influence the strength properties of the cast parts (among others) [5–11]. Therefore, an attempt was made in this study to determine the mechanical properties of samples cast from cobalt alloys containing the addition of process scrap.

2. TEST MATERIAL AND METHODOLOGY

Two cobalt alloys used in dentistry for the manufacture of frame dentures were chosen for the study. The chemical composition of these alloys is shown in Table 1.

Table 1
Chemical composition of test alloys [12]

| Alloy | Chemical composition, wt.% | | | | |
|-------|----------------------------|----|-----|-----|-----|
| | Co | Cr | Mo | Ta | Si |
| A | 64.6 | 29 | 4.5 | – | – |
| B | 62.0 | 30 | 5.5 | 1.2 | 1.2 |

From the selected alloys, cylindrical specimens with diameter $\varphi = 5$ mm and length $l = 80$ mm were cast in a dental prosthetics laboratory. The charge was composed of pure primary materials (samples labeled A1 and B1) and pure primary materials mixed with the addition of process scrap introduced in different amounts (samples labeled A2–A4 and B2–B4). The percent content of the introduced process scrap is shown in Table 2.

Table 2
Percent content of process scrap added to test alloys

| Sample designations | | Content of process scrap added to test alloys, % |
|---------------------|-------|--|
| A1 | B1 | – |
| A2_25 | B2_25 | 25 |
| A3_50 | B3_50 | 50 |
| A4_75 | B4_75 | 75 |

From the investment cast rod-shaped test pieces, specimens were prepared for the examination of non-metallic inclusions and the performance of a static tensile test.

Specimens for the evaluation of non-metallic inclusions were after cutting, grinding, and polishing examined under a Neophot 32 light microscope at 400 \times magnification.

The mechanical properties of the selected cobalt alloys were determined in a static tensile test performed on an Instron 5566 testing machine. The specimens were stretched at room temperature at a constant strain rate of 10^{-4} 1/s.

The fractures formed during specimen failure were examined under a JSM 7100F scanning electron microscope. The observations were conducted at magnifications ranging from 100 to 500 \times .

3. RESULTS AND DISCUSSION

Figure 1 shows the non-metallic inclusions present in the examined alloys. The observed precipitates are characterized by different shapes (globular and irregular), different sizes, and an uneven distribution on the examined surfaces.

Studies carried out by light microscopy did not reveal any major influence of the process scrap content on changes in the morphology of the inclusions present in the test samples.

The results of the static tensile test have shown that failure of the specimens occurred at different points in the measurement area, irrespective of the amount of process scrap added to the examined material.

From the stress-strain curves plotted during tensile testing (see sample diagram in Figure 2), it follows that the tested materials have no yield point.

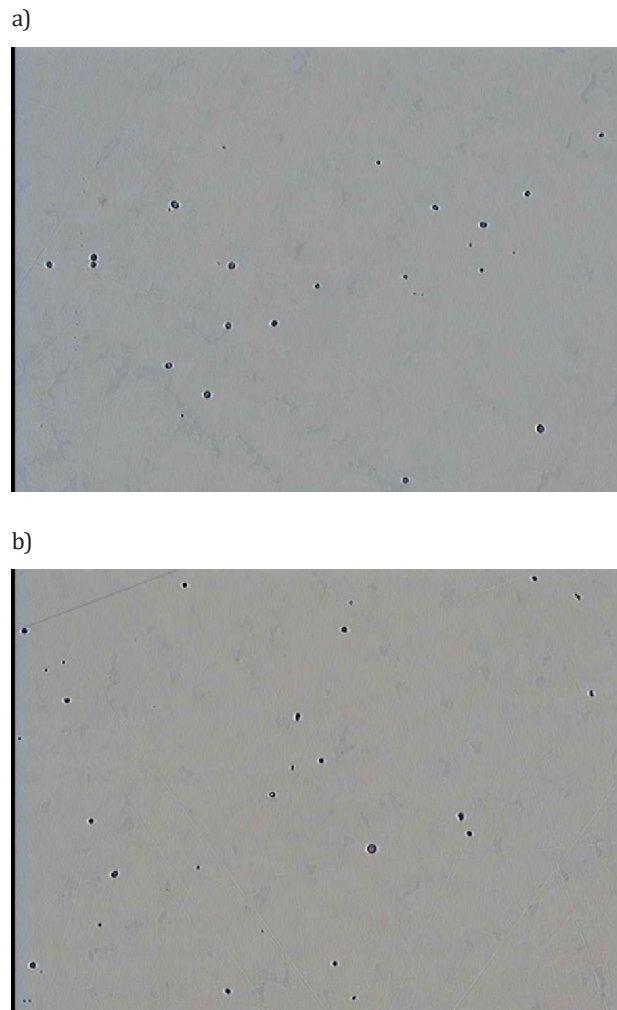


Fig. 1. Examples of non-metallic inclusions present in selected samples: sample A2_25 (a); sample B2_25 (b) light microscopy, magnification 400 \times

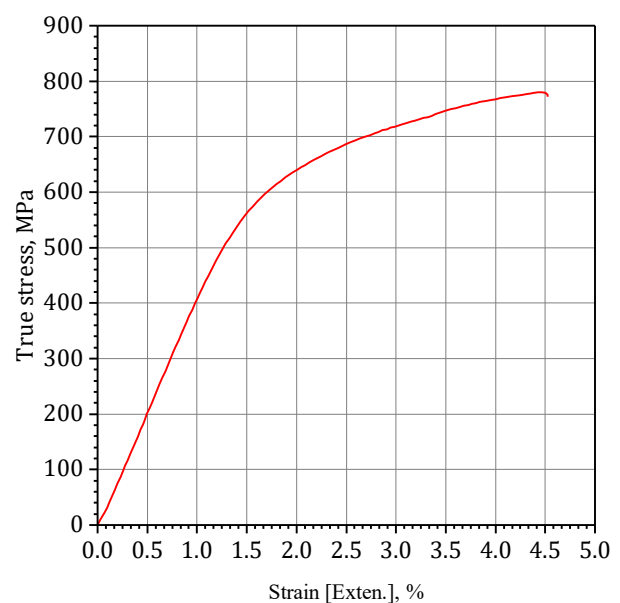


Fig. 2. Example of stress-strain curve plotted for investigated alloy

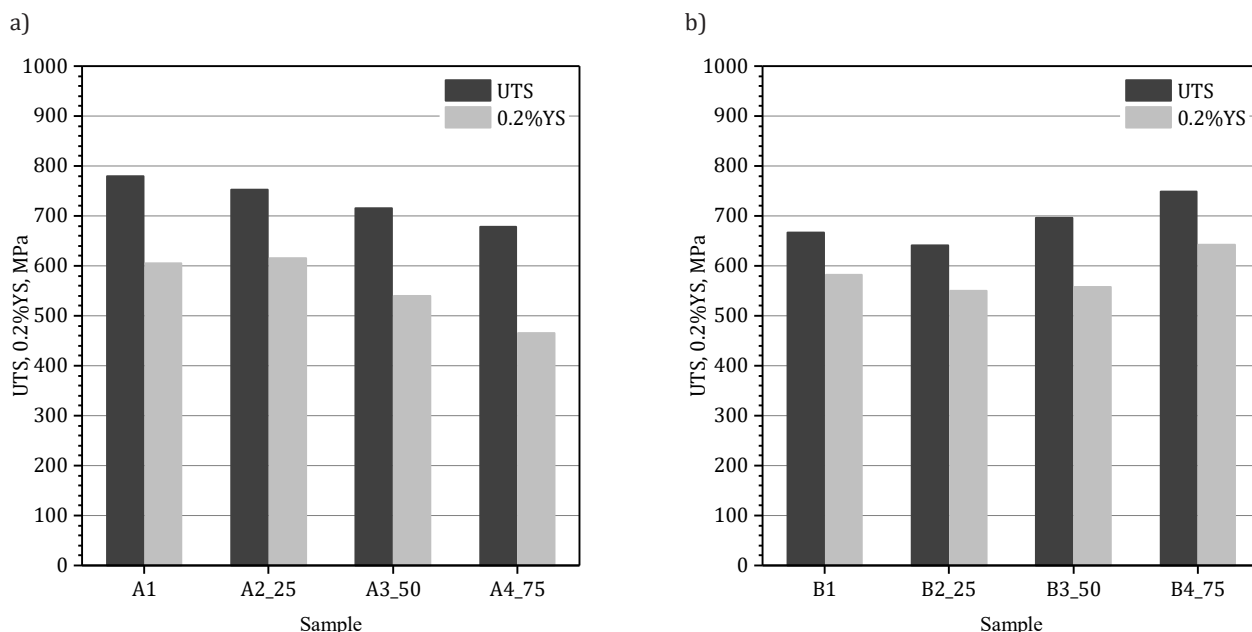


Fig. 3. Tensile strength UTS and yield strength 0.2%YS changing in tested alloys with changing scrap metal addition – Alloy A (a) and Alloy B (b)

Mechanical properties of the samples subjected to static tensile test are shown in Figures 3 and 4 and summarized in Table 3.

Table 3
Mechanical properties of the tested cobalt alloys

| Sample | UTS, MPa | 0.2%YS, MPa | EL, % |
|--------|----------|-------------|-------|
| A1 | 779 | 605 | 2.58 |
| A2_25 | 752 | 615 | 2.16 |
| A3_50 | 716 | 540 | 1.66 |
| A4_75 | 678 | 466 | 2.00 |
| B1 | 667 | 582 | 0.75 |
| B2_25 | 641 | 550 | 1.50 |
| B3_50 | 696 | 558 | 2.57 |
| B4_75 | 749 | 642 | 3.75 |

The obtained mechanical properties of the alloys tested differ greatly from the values given in the literature [12].

Based on the obtained data (Fig. 3a), it was found that the mechanical properties of the tested materials decreased with an increasing scrap metal content in the alloy (the only exception is the yield strength obtained in the sample designated as A2_25).

With the introduction of 25% of process scrap, the tensile strength of the material designated as B was lower than the strength of the starting alloy (Fig. 3b). Samples containing 50% and 75% of process scrap in their composition were characterized by tensile strengths higher than the strength of the starting material.

The yield strength of the samples containing 25% and 50% of process scrap was lower than the yield strength of the starting material. The highest yield strength was achieved by the material designated as A4_75 containing 75% process scrap. Except for the alloy sample containing 75% process scrap, the elongation of the material designated as A decreased with an increasing content of the added scrap (Fig. 4). In contrast, the elongation of the material designated as B increased with an increasing content of process scrap. To explain the surprising impact of the increase in the amount of scrap introduced into the alloys (primarily Alloy B) on the improvement of tensile strength and elongation, further tests should be carried out.

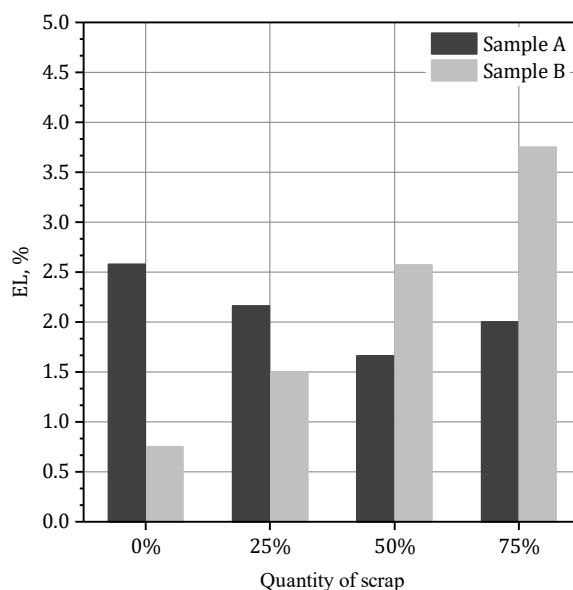
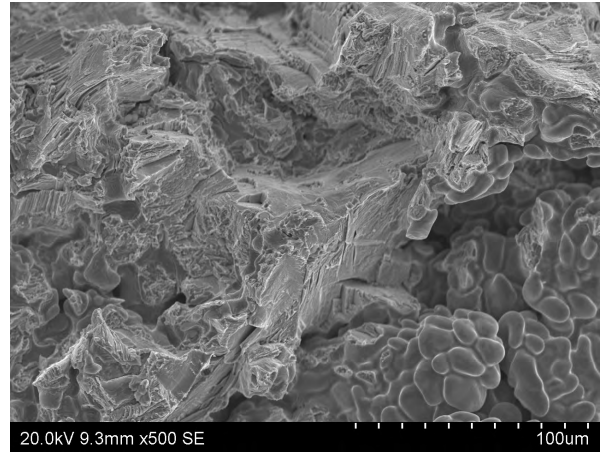
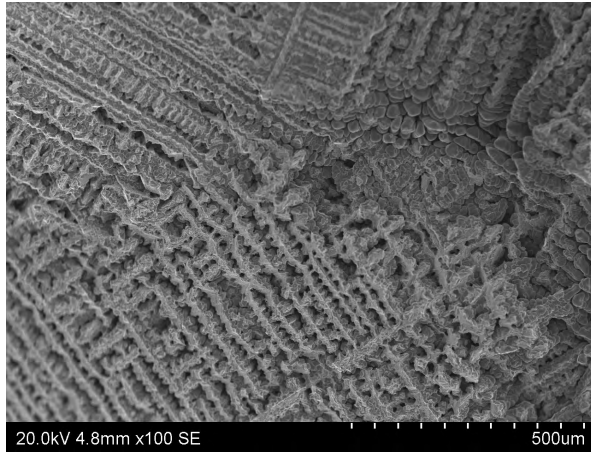


Fig. 4. Elongation changing in tested alloys with changing scrap metal addition

a)



b)

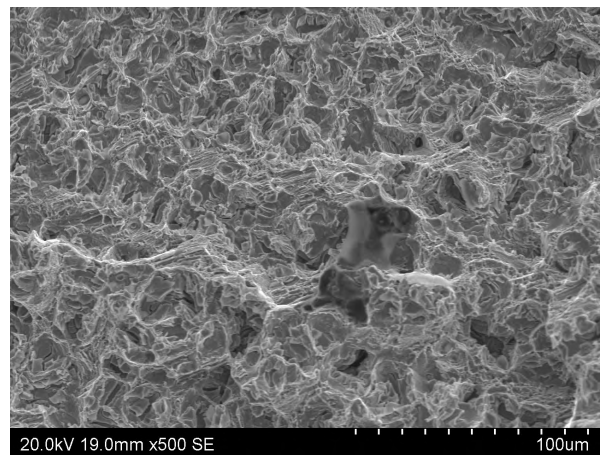


Fig. 5. Sample images of fractures formed in alloys during static tensile test – Alloy A (a) and Alloy B (b)

Figure 5 compares the SEM images of the fractures. Detailed examinations of the fractures formed during the static tensile test have revealed a dendritic pattern visible at low magnifications as well as shrinkage porosity occurring in the sample interior.

The observed fractures have different natures (ductile or transcrystalline). In some areas, sharp edges, large corrugations, and recesses occur.

4. CONCLUSIONS

The results of the studies lead us to the following conclusions:

1. In all of the tested materials, there are non-metallic inclusions characterized by different shapes and distributions.
2. From the results of a static tensile test, it follows that the tested material has no yield point.
3. The mechanical properties of the samples subjected to the static tensile test are definitely inferior to the values given by the manufacturer.
4. The values of UTS, 0.2%YS, and EL decreased in the tested Alloy A with an increasing content of process scrap.

5. Adding process scrap to the alloy designated as B makes the strength properties of this alloy decrease at first, followed by an increase. The elongation of the alloy designated as B increases with an increasing addition of process scrap. The maximum mechanical properties were obtained in the alloy designated as B4_75.

6. Factographic studies have revealed the presence of shrinkage porosity in the central part of the samples.

7. The examined fractures are of a ductile or transcrystalline nature.

Acknowledgements

The study was done as part of the bachelor's thesis of Dęsoł B. (2017). *Badania właściwości mechanicznych stopów kobaltu. AGH University of Science and Technology.*

REFERENCES

- [1] ISO 6871-1:1994 Dental base metal casting alloys – Part 1: Cobalt-based alloys.
- [2] Augustyn-Pieniążek J., Łukaszczyk A., Szczurek A. & Sowińska K. (2013). Struktura i własności stopów dentystycznych na bazie kobaltu stosowanych do wykonywania protez szkieletowych. *Inżynieria Materiałowa*, 34(2), 116–120.

- [3] Surowska B. (2009). *Biomateriały metalowe oraz połączenia metal-ceramika w stomatologii*. Lublin: Wydawnictwo Politechniki Lubelskiej.
- [4] Marciniak J. (2013). *Biomateriały*. Gliwice: Wydawnictwo Politechniki Śląskiej.
- [5] Surowska B., Beer K., Bienias J. (2011). Wpływ recyklingu na strukturę i właściwości wytrzymałościowe odlewniczego stopu kobaltu stosowanego w stomatologii. *Acta Mechanica et Automatica*, 5(3), 119–123.
- [6] Al-Ali A.A. (2007). Evaluation of Macrohardness of Recasted Cobalt-Chromium Alloy. *Al-Rafidain Dental Journal*, 7(1), 111–117.
- [7] Hajduga M., Puchalik A. (2009). Oszacowanie przydatności stopu Heraenium NA po przetopieniu w kontekście badań strukturalnych. *Nowoczesny Technik Dentystyczny*, 3, 56–60.
- [8] Henriques G.E.P., Consani S., de Almeida Rollo J.M.D., Andrade e Silva F. (1997). Soldering and remelting influence on fatigue strength of cobalt-chromium alloys. *The Journal of Prosthetic Dentistry*, 78, 146–152.
- [9] Majewski S., Opoka W., Gacek S. (1991). Właściwości stopu ćwiczebnego w zależności od postaci składników wyjściowych i wielokrotności odlewów. *Protetyka Stomatologiczna*, XLI(4), 192–198.
- [10] Pierzynka R., Marciniak S., Klimek L. (2010). Wpływ liczby przetopień na właściwości mechaniczne stopu DUCINOX. *Nowoczesny Technik Dentystyczny*, 2, 22–24.
- [11] Beer K., Walczak M., Surowska B., Borowicz J. (2012). Wpływ powtórnego przetapiania na właściwości mechaniczne i mikrostrukturę odlewniczego stopu kobaltu. *Inżynieria Materiałowa*, 33(5), 473–476.
- [12] Nadolski M., Łagiewka M., Konopka Z., Zyska A., Golański G. (2015). The influence of remelting on the quality of prosthetic cobalt alloys. *Archives of Foundry Engineering*, 3, 53–58.

Impact of Density Degree and Grade of Inorganic Binder on Behavior of Molding Sand at High Temperature

Mateusz Stachowicz^{a*}, Patrycja Paduchowicz^a, Kazimierz Granat^a

^a Wrocław University of Science and Technology, Department of Foundry, Plastics, and Automation, Łukasiewicza 7–9, 50-371 Wrocław, Poland

*e-mail: mateusz.stachowicz@pwr.edu.pl

Received: 8 August 2017/Accepted: 16 October 2017/Published online: 9 November 2017

This article is published with open access at AGH University of Science and Technology

Abstract

This paper discusses the impact of high temperatures (up to 900°C) on molding and core sand with inorganic binders selected from among the group of unmodified grades of hydrated sodium silicate (water-glass). Molding sands with medium quartz sand were made under laboratory conditions and compacted at the different energy inputs necessary for obtaining various apparent densities (ρ_a). Due to the different composition and apparent density of molding mixtures hardened via microwaves at a frequency of 2.45 GHz, it was possible to assess their deformation (L) at a high temperature above the binder's eutectic temperature. For this purpose, an apparatus for hot distortion tests was used whose construction and equipment allows us to measure the thermoplastic deformations in molding sand in many aspects; i.e., in its time of annealing. The article proposes new possibilities of interpreting the hot distortion phenomena in comparative studies of molding materials and mixtures. The application of this new measurement method revealed the differences between molding mixtures made with five inorganic binders with a molar module ranging from 2.0 to 3.4 and apparent density ranging from 1.34 to 1.57 g/cm³. It was established that distortions under the influence of high temperatures last the longest in molding sand with a binder with the highest molar module (3.4). Research also revealed that the density of molding sand is significant for increasing/decreasing the rate of thermoplastic deformations following the heating of samples only if the molding sand includes binders with a molar module of between 3.0 to 3.4. For molding sand with binders with molar modules from 2.0 to 2.5, it was established that this is excessively susceptible to thermoplastic deformation.

Keywords:

foundry, hydrated sodium silicate, hot-distortion, thermal deformation, molding sands

1. INTRODUCTION

If properly manufactured, casts should have the least-possible number of casting faults. It is expected that casts should be cost-effective and environmentally friendly. For the best effects, it is essential to select the proper composition of molding sand and correctly manufacture the mold and core [1, 2]. The new molding materials offered on the market at present are becoming better and better, as their quality and properties meet the strictest requirements. However, the requirements cannot guarantee that the casts are made without defects. The selection of an appropriate binder considerably affects the resistance of molding sand to jets of liquid metal. Research [3, 4] carried out with the use of binding materials like furan resins and water-glass demonstrated that it is more effective to use inorganic binders than organic ones. The technology of manufacturing molding and core sands and the molding parameters are also of importance. Among the reasons behind casting faults are the improper density of molding sand and the failure to adjust this parameter to the process of pouring and solidifying the casting alloy [1–4].

Quoting [5], the density degree of molding sand is a parameter dependent on the material properties and initial density degree. Proper distribution of density in the mold or core is affected by external and internal friction and elastic deformation at high temperature, among others. They may cause some resistance when a part is pulled out of the mold, which may in turn bring about deformations inside the mold cavity. The proper density of molding sand (which can also be expressed by another parameter – apparent density) ensures the required surface smoothness and casting dimension tolerance. In the process of densifying by pressing, for example, molding sand should be liquid to such an extent that it allows free movement from the areas of greater mold density to areas of smaller density [2].

If the density of molding sand increases, a greater shear force is needed to move the neighboring layers (which is particularly important and even desired for the manufacturing of casting cores); however, this eventually reduces casting surface roughness. The density degree of the molding sand and the shape and size of the matrix grains exert a considerable influence on mold or core permeability [6].

If, however, the density of the molding sand is improper and too low, it leads to the erosion of the mold surface layers and may bring about friability. The extent of wear detected in molding sand, including that with water-glass [7], depends on the angle of the liquid metal jets on the wall of the mold cavity as well as its temperature, dynamics, and pouring time. The defects caused by the insufficient density of molding sand include sand contamination and liquid metal penetration into the pores of the molding sand, lowering the casting surface quality. As a result of the excessive deformations inside the mold cavity, shape defects and burns occur [7, 8]. In order to eliminate such faults, protective coatings are applied [9–11]; however, this prolongs the time of mold preparation and impedes the process of matrix regeneration. The application of popular alcohol-based coatings has a negative effect on the environment due to the fact that, when the mold is dried before pouring, dangerous vapors and gases are released.

In molding sand with hydrated sodium silicate (water-glass), mold erosion is less intensive than in molding sand with organic binders; however, the area affected by the erosion is greater [7, 8]. Therefore, for this type of molding sand, it becomes necessary to use protective coatings in order to reduce corrosion pits and burns [4]. The coating thickness is also worth mentioning. Study [8] shows that, in the case of coatings applied on molding sand with water-glass, the thickness of the layer is of particular importance. Moreover, the casting quality largely depends on the phenomena that take place in the mold at the time liquid metal is poured into it (when the temperature is at its highest level). Then, thermal and mechanical deformations occur that affect the dimensional accuracy and casting surface smoothness.

Therefore, interesting from the point of cast quality is the identification of all phenomena associated with the impact of liquid metal on the elements of the casting mold cavity.

Helpful are tests based on a broadly understood analysis called “thermal” or “hot” distortion [11–13]. However, at the moment of writing the article, this method is not standardized nor determined by the relevant standards. As a result of the non-standardized measuring method, researchers are able to use a “hot-” or “thermal-” distortion apparatus to study the phenomena of deformation for various purposes as well as introduce them by their modifications and improvements, like in the DMA Hot Distortion Tester [11], Hot Distortion Plus® [14] method, or Hot Distortion Tester for the samples sized $5.24 \times 2.54 \times 1.27$ cm described in [15].

As opposed to the common analyses determining whether a given type of molding sand can be used in a production process, hot distortion tests (HDT) take into consideration not only the strength properties but also the thermal phenomena that largely influence the final casting shape, dimensional accuracy, and smoothness. During the pouring of the liquid metal into the mold, the alloy contact and intensively heats the mold cavity walls. As a result of the high temperature and mechanical stress, negative phenomena occur in the molding sand: thermal deformation, thermal and mechanical destruction, and thermoplasticity. These may damage the mold or core structure, which depend on the molding mixture components [11–17]. The extent of the distortions that emerged during the pouring of the liquid metal may be modified by means of special plasticizers added to the binders. These enhance the elasticity of the molding and core sand. Previous studies have confirmed the positive influence of collagen plus alkali silicate [15] on the properties of molding sand or polycaprolactone [18] on the properties of molding sand with phenol-furfural resin. Another method for improving the strength properties of molding sand at high temperatures consists of applying coatings on the cores. The effectiveness of these methods is confirmed by hot distortion analyses made for cores with a hydrated sodium silicate [19].

The strength of physically cured molding sand with hydrated sodium silicate at an ambient temperature is higher than that of bentonite molds and comparable [20, 21] to molding sand with organic binders. However, the pouring of liquid metal causes greater damage in molding sand with hydrated sodium silicate as the binder [7, 22]. In order to explain this phenomenon, it seems the analyses of molding sands at high temperatures will be of key importance.

2. RESEARCH METHODOLOGY

The molding sand used for the purposes of this study was made of dried medium quartz sand with a grain size of 1K 0.20/0.315/0.16 (according to norm PN-85/H-11001) from a Polish mine (Grudzeń Las) and five unmodified grades of hydrated sodium silicate produced in a chemical plant called ‘Rudniki’ S.A. (Tab. 1). Each time, 1 kg of molding sand was prepared by means of a planetary mixer: to 100 weight parts of the matrix, 0.5 weight parts of water were added [21]; then, after 60 s of mixing, 1.5 weight parts of the selected binder were added and mixed for 180 s.

Table 1
Physico-chemical properties of five grades of hydrated sodium silicates used for preparation of molding sands

| Grade of hydrated sodium silicate/ Type of molding sand | Molar module ($\text{SiO}_2/\text{Na}_2\text{O}$) | Oxide contents ($\text{SiO}_2 + \text{Na}_2\text{O}$), min. % | Measured oxide contents ($\text{SiO}_2 + \text{Na}_2\text{O}$), % | Measured density (20°C), g/cm ³ | Absolute viscosity min., P |
|--|--|---|--|---|----------------------------------|
| 137 / MS137 | 3.4 | 35.0 | 36.3 | 1.37 | 1 |
| 140 / MS140 | 3.0 | 36.0 | 39.4 | 1.42 | 1 |
| 149 / MS149 | 2.9 | 42.5 | 44.3 | 1.51 | 7 |
| 145 / MS145 | 2.5 | 39.0 | 41.5 | 1.47 | 1 |
| 150 / MS150 | 2.0 | 40.0 | 43.5 | 1.52 | 1 |

The samples with the dimensions of $120 \times 25 \times 6$ mm ($l \times b \times h$) to be investigated in terms of distortions at higher temperatures were compacted by means of an LU-1 laboratory rammer. A weight of 6.667 kg was dropped a different number of times from a fall height of 50.3 mm in order to obtain various density. In this research, the samples were compacted two (II), three (III), or five times (V) using the rammer.

The molded samples were then hardened with electromagnetic waves of a frequency of 2.45 GHz and power of 1000 W in the chamber of a microwave furnace by Plazmatronika (with a capacity of 32 dm³) equipped with one magnetron and the load-rotation feature. The selected heating time of 240 s regardless of the various density degrees of the samples (ranging from 1.05 to 1.40 g/cm³) ensured the effective dehydration of the molding sand in its whole volume [23]. The analyses started from a mass stabilization to the nearest 0.01 g by means of an Ohaus PA4102CM/1 scale. The density degree was expressed as the apparent density (ρ_0); i.e., as the ratio of the mass of each sample after curing and cooling-down to the volume calculated on the basis of its dimensions. For the purposes of the hot distortion test (HDT), a DMA apparatus made by Polish company Multiserw-Morek was used for examining the high temperature phenomena in molding sand. This HDT device [24] has two ceramic heaters and a max. temperature of heating ca. 990°C measured by K-type thermocouples.

The sample is placed in a special support and heated conventionally from two sides in its middle part (see Fig. 1). Thermal energy from both ceramic heating elements increases the environment temperature up to ca. 900°C, causing distortion.

On the free end of the fitting, a sensor is placed that registers any changes in the sample location against time during annealing at ca. 900°C. Depending on the grades of the molding sand and binder, the phenomenon of molding sand thermoplasticity occurs or not. Usually, deformation occurs in the direction of the applied load and the sensor located at the end of the sample (Fig. 1).

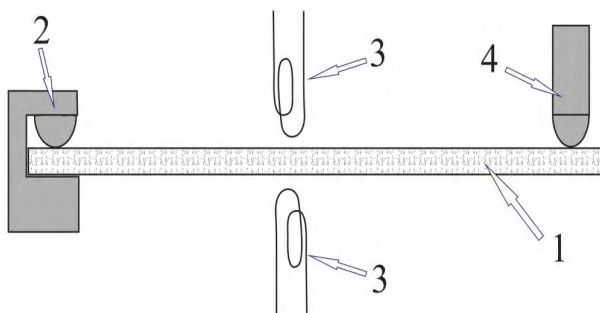


Fig. 1. Diagram of thermal deformation measuring stand: 1) sample of molding sand; 2) support with grip; 3) heaters; 4) load (sensor) [24]

An annealing temperature set at $900^\circ\text{C} \pm 10^\circ\text{C}$ is above the temperature of phase transitions [25, 26] observed for commercial grades of sodium silicate. In previous studies [27], an unfavorable flow of the melted binder was observed at temperatures above 750°C.

This study attempts to explain the phenomenon of the increased erosion of sodium silicate molding sands due to the effect of metal poured into cavity.

3. RESULTS

The first value under investigation was the average apparent density expressed in g/cm³. The mass of the samples (cured and cooled for the purposes of the distortion tests) was compared to their capacity of 18 cm³; the results of which are demonstrated in Figure 2.

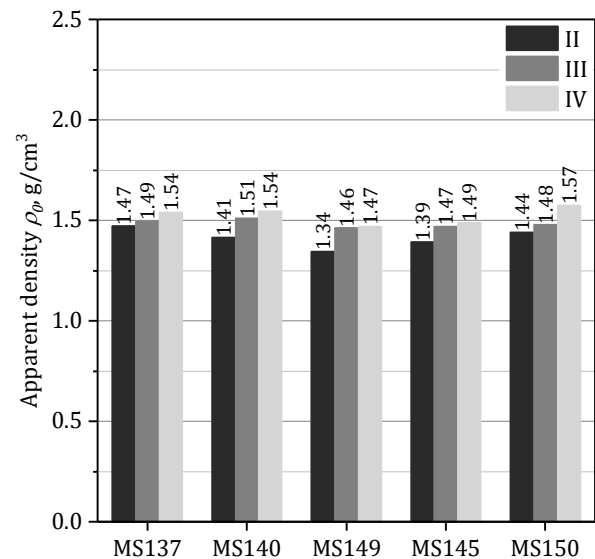


Fig. 2. Apparent density of cured molding sand with five grades of hydrated sodium silicate

The analysis reveals that the apparent density of the molding sand (MS137 – MS150) ranges from 1.34 to 1.57 g/cm³ (Fig. 2). Due to the compacting method, it was feasible to differentiate between the apparent density of the molding sands with five grades of binders. As we know [28, 29], this is an important parameter for molding mixtures because of the interdependence between the increase/decrease in the apparent density of molding sand with a hydrated sodium silicate of 0.1 g/cm³ and a constant (40%) increase/decrease in their strength. Figures 3–7 show measurement graphs for the samples subjected to two-sided heating near the DMA elements heated up to 900°C (see Fig. 1).

Near the middle of the sample section, the ambient temperature in close proximity to the sample was recorded. An increase of 1°C set the beginning of deformation (L) recording. Unfortunately, the originally adopted method of testing the deformation (L) of the sample as a function of rising temperatures proved to be rather inaccurate. According to the indications of the environment temperature measuring element, the phase transition of the binder was already at 180–220°C, which was not observed in the research [25–27]. It was decided to present the results of thermal deformation as a function of time during the both-side heating of the samples (Figs. 3–7).

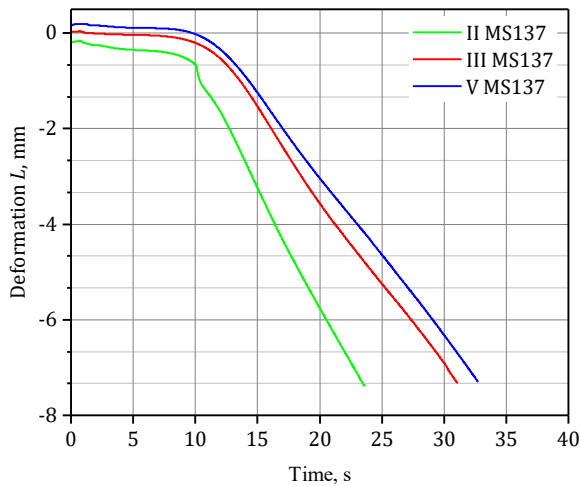


Fig. 3. Measurement results of hot distortion tests for molding sand with hydrated sodium silicate grade 137 densified two-, three-, or five-fold times

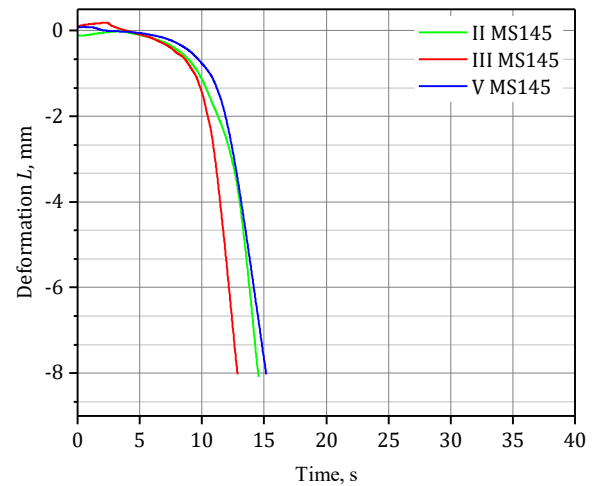


Fig. 6. Measurement results of hot distortion tests for molding sand with hydrated sodium silicate grade 145 densified two-, three-, or five-fold times

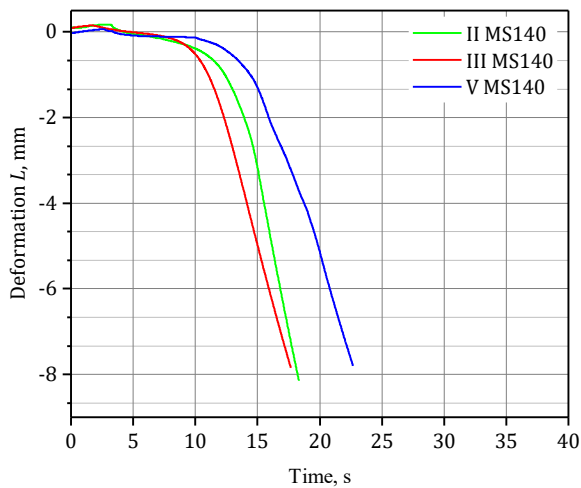


Fig. 4. Measurement results of hot distortion tests for molding sand with hydrated sodium silicate grade 140 densified two-, three-, or five-fold times

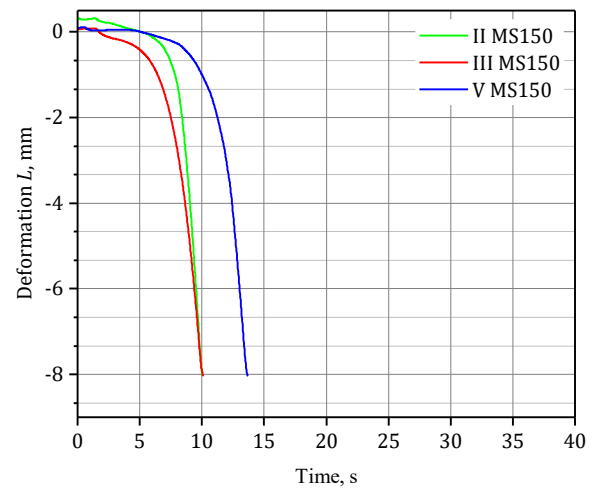


Fig. 7. Measurement results of hot distortion tests for molding sand with hydrated sodium silicate grade 150 densified two-, three-, or five-fold times

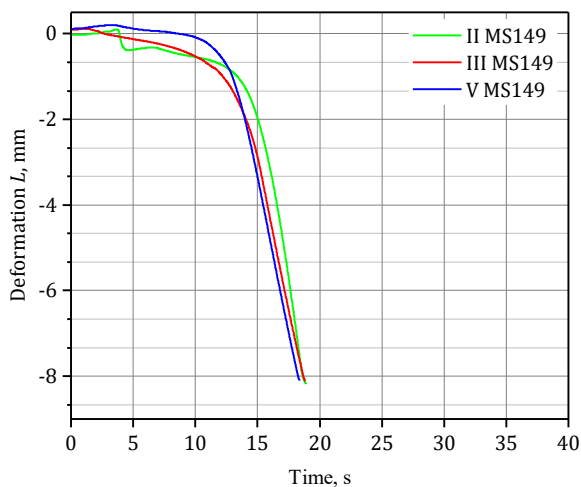


Fig. 5. Measurement results of hot distortion tests for molding sand with hydrated sodium silicate grade 149 densified two-, three-, or five-fold times

The analysis of distortion changes revealed that all types of molding sand with different grades of hydrated sodium silicate cured in an electromagnetic field have low heat expansion. After heating the samples on both sides, they became plasticized in a short amount of time. Each measurement was interrupted after the sample distortion exceeded 8 mm. None of the samples was fractured during the heating process. It was established that the thermal deformations lasted the longest for the molding sand with a binder of a maximum molar module of 3.4 (Fig. 3).

In the case of this type of molding sand, the influence of a diversified apparent density on the speed with which the sample end moves under the weight of the sensor is also visible. Sample MS137 compacted five times to a density of 1.54 g/cm³ (Fig. 3) showed the least thermoplasticity (the slope of the deformation curve to the time axis was the least).

A similar phenomena of the slowing down of the process of molding sand plasticizing under the influence of high temperatures was detected for hydrated sodium silicate with a molar module of 3.0 – MS140 (see Fig. 4). The deformation graphs (Fig. 5) demonstrate a tendency similar to that for binders 137 and 140; i.e., a tendency to impede the process of plasticizing the molding sand with grade 149 hydrated sodium silicate. However, it was established that the thermal deformation is not sensitive to diversified density (Fig. 2) for this molding sand – MS149. The types of molding sand with the binders of grades 145 (Fig. 6) and 150 (Fig. 7) can be deemed as susceptible to excessive thermoplasticity on the basis of deformation changes, while the diversified apparent density of the molding sand exerted no influence on the rate of changes. The exception is MS150 with the highest measured apparent density (1.57 g/cm³), in which the resulting density has a delayed process of sample plasticization. It should be noticed, however, that all types of molding sand had low contents of binders (1.5 %wt.), which may be of significance for the speed at which the bridges binding the matrix grains plasticize. When cooled down to the ambient temperature, all of the samples crumbled in the middle, which confirms findings [22, 27, 30] from recent research into microwave heating used for the curing of molding sand with hydrated sodium silicate.

4. CONCLUSION

An analysis of the thermal deformation of molding sand with hydrated sodium silicate cured by means of microwave heating revealed that it is the grade (molar module) of the binder that is essential; moreover:

For the molding sand with binders of molar modules ranging from 3.0 to 3.4 (Fig. 3), thermal deformations lasted the longest. The study also proved that, for these binders, the density of the molding sand is essential for increasing/decreasing the speed of thermoplastic deformation resulting from the heating of the samples.

For molding sand with a binder grade 149 and of a molar module of 2.9, a tendency to impede the process of plasticizing the molding sand was established (though the distortion is not affected by diversified density).

The most-common types of molding sand in the foundry industry (i.e., molding sands MS150 and MS145 with binders of molar modules from 2.0 to 2.5 [grades 150 and 145]) show excessive thermoplasticity.

The Multiserw-Morek DMA device allows us to adopt its basic HDT measurement functions for the precise comparative research of molding mixture behavior at high temperatures to reduce the negative effect of cavity erosion. The study proved that precise HDT measurements are possible while the temperature of the sample environment is well stabilized.

Further research should be carried out with a different content of binders containing hydrated sodium silicate and other physical and physico-chemical methods of curing in order to select the optimum environment-friendly technology of molding and core sand.

Acknowledgements

The research has been financially supported by the Wrocław University of Technology with grants for statutory activity No. 0402/0165/16.

REFERENCES

- [1] Lewandowski J.L. (1997). *Tworzywa na formy odlewnicze*. Kraków: Wydawnictwo Akapit.
- [2] Szreniawski J. (1968). *Piaskowe formy odlewnicze*. Warszawa: Wydawnictwa Naukowo-Techniczne.
- [3] Mocek J., Zych J., Chojecki A. (2004). Study of erosion phenomena in sand moulds poured with cast iron. *International Journal of Cast Metals Research*, 17(1), 47–50.
- [4] Zych J., Mocek J. (2002). Zjawisko erozji w formach wykonywanych z mas ze spoiwami chemicznymi. *Archives of Foundry*, 2(3), 155–162.
- [5] Biernacki R., Perzyk M., Kozłowski J. (2006). Modelowanie rozkładu stopnia zagęszczenia masy formierskiej z wykorzystaniem systemów uczących się. *Archiwum Odlewnictwa*, 6(18), 477–482.
- [6] Gierek A. (1968). *Teoretyczne podstawy określania wielkości energii zagęszczania mas formierskich oraz jej wpływ na niektóre własności form odlewniczych*. Mechanika, z. 33, Gliwice: Wydawnictwo Politechniki Śląskiej, zeszyt naukowy nr 215.
- [7] Mocek J. (2003). Proces erozji form piaskowych ze spoiwem-szkłem wodnym. *Archives of Foundry*, 3(10), 23–30.
- [8] Zych J., Mocek J. (2015). Destruction of moulding sands with chemical binders caused by the thermal radiation of liquid metal. *Archives of Foundry Engineering*, 15(4), 95–100.
- [9] Jamrozowicz Ł., Zych J., Kolczyk J., Wróblewski D. (2014). Rola kształtu powierzchni formy w procesie wysychania wybranych powłok ochronnych. *Archives of Foundry Engineering*, 14(spec. iss. 2), 39–44.
- [10] Liu F.C., Fan Z.T., Liu X., Huang Y., Jiang P. (2016). Effect of surface coating strengthening on humidity resistance of sodium silicate bonded sand cured by microwave heating. *Materials and Manufacturing Processes*, 31(12), 1639–1642.
- [11] Jakubski J., Dobosz S.M. (2007). The thermal deformation of core and moulding sands according to the hot distortion parameter investigations. *Archives of Metallurgy and Materials*, 7(52), 421–427.
- [12] Morgan D., Fashman E.W. (1975). The BCIRA hot distortion tester for quality in production of chemically bonded sands. *AFS Transaction*, 75(91), 73–80.
- [13] Rodriguez J., Keil M., Ramrattan S., Krysiak M.B. (1998). Industry and academia collaboration for a thermal distortion tester for sand-binder systems. In: *Proceedings of the 1998 Annual Conference Seattle, Washington*. American Society for Engineering Education.
- [14] Ignaszak Z., Prunier J.B. (2013). Synergy of practical knowledge of moulding sands reclamation in heavy casting foundry of iron alloys. *Archives of Foundry Engineering*, 13(3), 30–36.
- [15] Fox J.T., Cannon F.S., Brown N.R., Huang H., Furness J. (2012). Comparison of a new, green foundry binder with conventional foundry binders. *International Journal of Adhesion & Adhesives*, 43, 38–45.
- [16] Dobosz S.M., Gieniec A. (2002). Wpływ rodzaju osnowy na zjawiska wysokotemperaturowe w masach rdzeniowych. *Archives of Foundry*, 2(2), 33–38.
- [17] Jakubski J., Dobosz S.M., Jelinek P. (2005). The influence of the protective coating type on thermal deformation of casting cores. *Archives of Foundry*, 5(5), 164–169.
- [18] Major-Gabryś K., Grabarczyk A., Dobosz S.M., Drożyński D. (2016). Wpływ dodatku materiału biodegradowalnego jako komponentu dwuskładnikowego spoiwa odlewniczych mas formierskich i rdzeniowych na właściwości spoiwa oraz mas z jego zastosowaniem *Prace Instytutu Odlewnictwa*, 16(4), 391–399.

- [19] Wildhirt E., Jakubski J., Sapińska M., Sitko S. (2017). Impact of penetration depth of protective coating on thermal deformation of masses determined by the hot distortion parameter. *Prace Instytutu Odlewnictwa*, 56(1), 51–57.
- [20] Jelinek P., Polzin H. (2003). Strukturuntersuchungen und Festigkeitseigenschaften von Natrium-Silikat-Bindern. *Giesserei-Praxis*, 2, 51–60.
- [21] Stachowicz M., Granat K., Palyga Ł. (2016). The effect of wetting agent on the parameters of dry moulding silica sands bonded with sodium water glass. *Prace Instytutu Odlewnictwa*, 56(1), 43–55.
- [22] Stachowicz M., Granat K., Nowak D. (2011). Application of microwaves for innovative hardening of environment-friendly water-glass moulding sands used in manufacture of cast-steel castings. *Archives of Civil and Mechanical Engineering*, 11(1), 209–219.
- [23] Stachowicz M. (2016). Effect of sand base grade and density of moulding sands with sodium silicate on effectiveness of absorbing microwaves. *Archives of Foundry Engineering*, 16(3), 103–108.
- [24] DMA Hot-Distortion tester for bonded sands – Multiserw-
-Morek instruction manual 2017.
- [25] Kracek F.C. (1930). The System Sodium Oxide-Silica. *The Journal of Physical Chemistry*, 34(7), 1583–1598.
- [26] Ryś M. (2007). Investigation of Thermodynamic Properties of Alkali Metals in Oxide Systems Relevant to Coal Slags. Unpublished engineering thesis, Rheinisch-Westfälischen Technischen Hochschule Aachen, Aachen, Germany.
- [27] Stachowicz M., Granat K., Nowak D. (2011). Influence of water-glass grade and quantity on residual strength of microwave-hardened moulding sands. Pt. 2. *Archives of Foundry Engineering*, 11(2), 143–148.
- [28] Zych J. (2005). Rola zagęszczania w technologii formy opartej na masach ze szkłem wodnym i spoiwami organicznymi. *Przegląd Odlewnictwa*, 55(2), 88–97.
- [29] Stachowicz M. (2017). The role of the densification of moulding sands with inorganic binders in the modeling of their strength obtained after microwave hardening. *Prace Instytutu Odlewnictwa*, 57(2), 103–113.
- [30] Stachowicz M., Granat K., Nowak D. (2011). Influence of water-glass grade and quantity on residual strength of microwave-hardened moulding sands. Pt. 1. *Archives of Foundry Engineering*, 11(1), 93–98.

Density Distribution and Resin Migration Investigations in Samples of Sand Core Made by Blowing Method

Rafał Dańko^{a*}, Łukasz Jamrozowicz^a

^aAGH University of Science and Technology, Faculty of Foundry Engineering, Reymonta 23, 30-059 Krakow, Poland
^{*}*e-mail: rd@agh.edu.pl*

Received: 1 September 2017/Accepted: 15 October 2017/Published online: 9 November 2017
This article is published with open access at AGH University of Science and Technology

Abstract

Resin migration in a core can occur during the core production process performed by blowing methods in which the core sand is transported into the core box as a two-phase sand-air flux characterized by various working parameters (working pressure, shooting time, volumetric concentration). This migration is the result of the resin being blown off from the matrix grain surfaces by compressed air. The methodology of the investigation of this effect developed at AGH University of Science and Technology is presented in this paper. The results of the resin migration tests obtained for cores made with cold-box technology at various working parameters of the shooting process are also shown.

Keywords:

core shooting, core blowing, molding sand, resin migration

1. INTRODUCTION

The blowing process [1–8] of molding sand compaction and its hardening (during which, a sand-air flux is introduced into a mold cavity and followed by successive flows of air and a hardening factor – one after another – into venting holes) is burdened with at least two disadvantages. The first one constitutes the diversification of the molding sand compaction within the core volume, especially visible when the sand is shot through individual shooting holes, since it leads to a significantly higher apparent density in the shooting hole axis. The second disadvantage is resin migration under the influence of air flux. This air flux is filtered via the porous medium into the venting holes.

It can be assumed that both aspects occur in all varieties of the core production technology based on shooting molding sands with liquid resins, hardened by gaseous factors. These aspects are especially important for sands with binders with a low viscosity, which characterizes, among others, the classic cold box technology (Ashland process). This is the subject of our investigations.

The discussed process is based on producing cores with the application of a gaseous hardener. The core sand contains 100 parts by weight of sand, 0.4–0.8 parts by weight of polyalcohol-benzyl-ether, and 0.4–0.8 parts by weight of polyisocyanate. Both the resin and polyisocyanate are low-viscosity liquids, usually mixed at a ratio of 1:1. This mixture reacts in the presence of the proper amino-catalyst blown through the core sand. The resin polymerization occurs in a few seconds. At the end of the hardening reaction, the unused amine shifts itself

to successive sand portions and catalyzes their reaction. After the total core hardening, amine is rinsed out by the cleaning air and then transferred to a neutralizing washer filled with sulfuric acid.

2. INVESTIGATIONS

The standard high-silica sand (100 parts by weight) from the Grudzeń-Las mine was used as the matrix in our investigations. For preparation of the molding sands, the phenol-formaldehyde resin (0.8 parts by weight) of the trade name Gasharz 6966 from the Hüttenes Albertus Company was applied. The second component of this binder was polyisocyanate (0.8 parts by weight) of the trade name Aktywator 7624 from the same company. As the catalyst of the reaction between both binder components, dimethyl-ethyl-amine (DMEA) was applied in the preparations of the cores, while amine of the trade name Katalizator GH3 was used in the investigations.

Core sands were prepared in a laboratory paddle mixer (type LM-R1). The core sand portion was 5 kg each time, which warranted the proper mixing of the components. The mixing time was 3 min. To begin with, the sand with the first part of the binder was mixed for 1.5 min.; then, the second part of the binder was added and mixed for the next 1.5 min.

The shaped elements on which the tests were performed were made by the experimental blower shown in Figure 1. The blowing machine is equipped with shooting chambers with a volume of 2.2 liters. The shooting chambers are equipped with heads that have three blowing nozzles (each of a diameter of 11 mm) and venting stoppers.



Fig. 1. Research stand with blowing machine

Due to the upper air supply (above the sand), it should be assumed that it meets the classification criteria concerning the blower and realizes the blowing process. The application of the experimental core box (Fig. 2) allowed us to make the shaped elements destined for testing the resin migration. The measurements were performed on the longitudinal shaped elements of dimensions $22.5 \times 22.5 \times 167$ mm prepared on a research stand. Three shaped elements were made in one cycle.

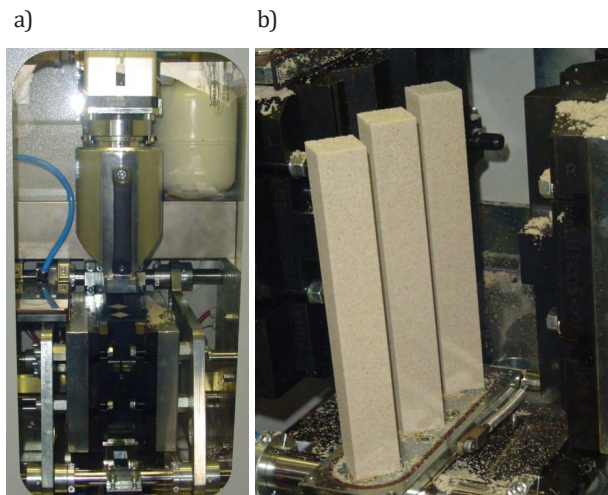


Fig. 2. Core box (a) and shaped elements (b) made of core sand

The prepared core sand was blown into the core box at air pressures (p) of 0.40, 0.45, 0.50, and 0.55 MPa while applying the following blowing times in each series: 0.5, 1.0, and 1.5 seconds. After core compaction, the gaseous catalyst was blown through the core with a pressure of 0.15 MPa. The time of blowing was 3 seconds. The amount of amine blown into the core box was approximately $1.7 \text{ cm}^3/\text{cycle}$ (for 420 g of core sand). After hardening, the cores were blown through by air for 17 seconds.

Measuring of the resin migration was performed as follows: compacted and hardened shaped elements made out

of the core sand were cut into 7 pieces with similar dimensions. The way of dividing these shape elements is presented in Figure 3. Then, each sample was crushed and weighed. Sample elements prepared in such a way were roasted in an M14 sylite furnace at a temperature of 850°C for 1 hour. After cooling, the sample was weighed again, and then the resin content was calculated according to equation [3]:

$$M = \frac{m_0 - m_1}{m_0} \times 100\% \quad (1)$$

where:

M – resin content in the given part of the shaped element, %;

m_0 – sample mass before roasting, g;

m_1 – sample mass after roasting, g.

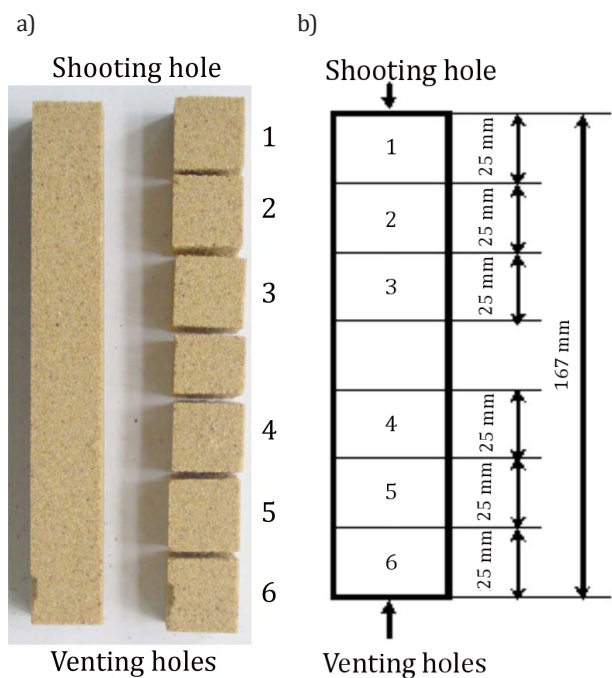


Fig. 3. Method of dividing sample of dimensions $22.5 \times 22.5 \times 167$ mm into elements for apparent density and binder content measurements: a) view of cut sample; b) scheme of division

The second testing series concerned the core sand apparent density measurements in the given piece of the shaped element. For this aim, the individual parts of the sample before crushing were measured by a slide caliper and weighed. The apparent density was calculated in the following way [3]:

$$\rho = \frac{m}{a \times b \times c} \quad (2)$$

where:

ρ – apparent density of the core sand, g/cm^3 ;

a, b, c – dimensions: width, thickness, height – respectively, cm;

m – sample mass, g.

3. RESULTS AND ANALYSIS OF MEASUREMENTS

The results of the resin content in the core sand sample at a pressure of 0.40 MPa are shown in Figure 4. The binder content in the core sand should be 1.6% and should be the same throughout the whole core volume.

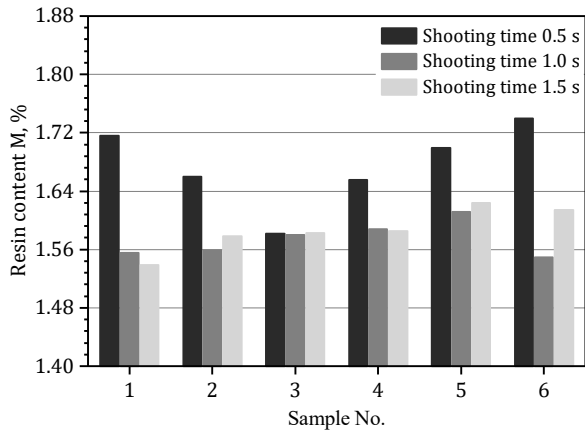


Fig. 4. Investigations of resin migration for core sand containing 1.6% resin, $p = 0.40$ MPa

Analyzing the diagram, it can be noticed that, for the shooting time of 0.5 s, the smallest binder content occurs in the middle part of the shaped element (sample elements Nos. 3 and 4). For Sample No. 3, this does not even reach 1.6%. Such a binder distribution causes a weakening in the shaped element middle part in the place where this element is most-susceptible to breaking. For shooting times of 1.0 and 1.5 seconds, the smallest amount of the binder occurs at both ends of the shaped element, which means at the shooting hole (Sample No. 1) and near the venting holes (Sample No. 2). Along with an increasing distance from the shooting hole, the binder content increases and achieves the maximum value in Sample No. 5.

The binder distribution in the core sand is caused by the air introducing this sand into the core box. In dependence of the process realization, the air causes a tearing away of the binder part from the sand grains and transfers them to the porous core channels in accordance with the flow direction. The small amount of binder at the end of the shaped element is caused by blowing out liquid resin from the venting hole range where, due to the air expansion, its flow rate increases. It should be also noticed that the binder content is only higher than 1.6% in Sample No. 5, while it is smaller for the remaining samples.

The data given in Figure 5 indicates that, after increasing the shooting pressure to 0.45 MPa, the binder distribution at the core length observed in the shaped elements for a pressure of 0.40 MPa and shooting times being 1.0 and 1.5 seconds, which is similar and occurs for all times of the core box filling. Certain differences can be found when the binder content in Sample No. 1 will be compared for both pressure values. In the case of the pressure of 0.45 MPa, the binder amount is lower by approximately 0.04%. A similar situation concerns the remaining samples.

Only in Sample No. 5 does the binder content exceed 1.6%; this is comparable with the amount obtained for the pressure of 0.40 MPa.

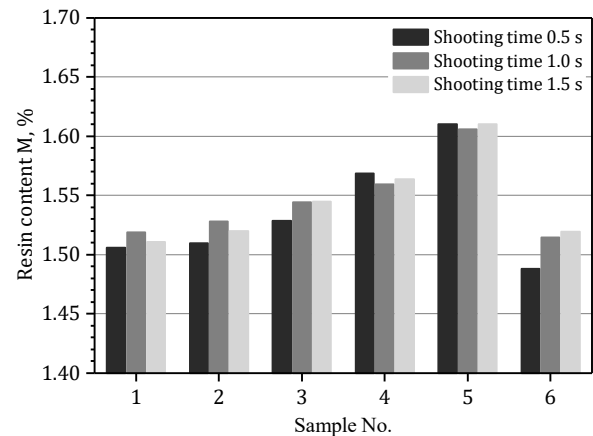


Fig. 5. Results of binder migration testing in longitudinal sample for core sand containing 1.6% resin, $p = 0.45$ MPa

The blowing of the core sand with a pressure of 0.50 MPa caused a similar binder distribution in the longitudinal sample. However, for a blowing time of 0.5 seconds, an increase of the binder content occurs nearer the shooting hole in Sample No. 4 while, for other times, it occurs in Sample No. 5. The binder content for this pressure is also lower in the individual samples than for pressures of 0.40 and 0.45 MPa. It should also be emphasized that, for a shooting time of 1.5 seconds, the binder content in Sample No. 1 is less than 1.5%. An analysis of the distribution of core sand compaction in the individual samples indicates that this distribution is uneven. The highest compaction occurs in the middle of the shaped element (Sample Nos. 3 and 4), while the lowest is at the ends (Sample Nos. 1 and 6).

The results of the investigations presented in Figure 6 indicate that the binder distribution on the core length is similar to the previous cases for shooting times of 0.5 and 1.0 seconds; i.e., the smallest binder amounts are at the ends of the shaped element (Sample Nos. 1 and 6).

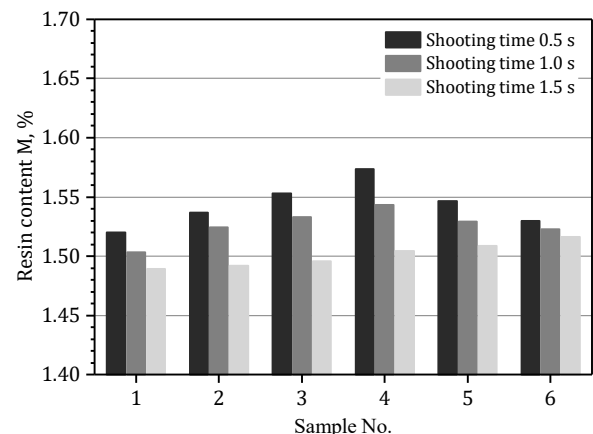


Fig. 6. Results of resin migration tests in longitudinal sample for core sand containing 1.6% resin, $p = 0.55$ MPa

The binder content increase (for these times) also occurs in Sample No. 4; however, its maximum value does not exceed 1.6%. A different binder distribution occurs for a shooting time of 1.5 seconds. In this case, the smallest binder content occurs at the shooting hole (Sample No. 1) and increases with an increasing distance from this hole. The highest binder content occurs at the venting hole (Sample No. 6). The general binder content for a shooting pressure of 0.55 MPa is the smallest when compared with the values obtained for lower blast pressures.

4. CONCLUSIONS

Summarizing the presented investigation results, it can be stated that, in the process of core production by blowing methods (blowing, shooting), the uneven distribution of sand compaction in the core is a reproducible effect. Regardless of the blowing pressure and blowing time, the highest compaction occurs in the blowing hole axis (middle of the core) and the lowest in places being at a distance from this axis. In the core ranges adjacent to the venting holes, a zone of better-compacted core sand occurs. The lower compaction degree of the sand at the core or sample ends forces an increased flow of the gas flux in the surface layers of the core due to the better permeability of the core sand being in these places.

The resin distribution in the shaped element (obtained by blowing the core sand into the core box), important for assessing the core sand strength, is not uniform but is subjected to certain regularities. The smallest amount of resin occurs in the part adjacent to the shooting hole, while the largest occurs in the vicinity of the venting holes. In addition, the influence of the shooting pressure on the resin content in the core sand is noticeable. It is especially visible for a shooting pressure of 0.55 MPa (Fig. 6). Along with an increase of the air-blast working pressure as well as a blowing-time increase, the resin content decreases (which

indicates that a certain resin amount is shifted to the surroundings by the air flux). The observed effect indicates the necessity of optimizing the blowing-process parameters in the direction of minimizing the working pressure and blowing time as well as the need for individual selection of these parameters for the given technology and core shape.

Acknowledgements

This work was supported by Polish NCN project UMO-2014/15/B/ST8/00206.

REFERENCES

- [1] Bakhtiyarov S.I., Overfelt R.A. (2003). CFD modeling and experimental study of resin-bonded sand/air two-phase flow in sand core making process. *Powder Technology*, 133, 68–78.
- [2] Ni C., Guo E., Zhang Q., Jing T. & Wu J. (2016). Frictional-kinetic modeling and numerical simulation of core shooting process. *International Journal of Cast Metals Research*, 29, 214–221.
- [3] Dańko J. (1995). An effect of the venting system on the core box filling ratio and the apparent core density structure. *Przegląd Odlewnictwa*, 3, 85–92.
- [4] Dańko J., Zych J., Dańko R. (2009). Diagnostic methods of technological properties and casting cores quality. *Archives of Metallurgy and Materials*, 54(2), 381–391.
- [5] Vidal V., Beauvais P., Leger-Delcourt E., Hossemand J.S., Sadon P. (2005). Pressure distribution during core production core blowing machines. *Fonderie Fondateur D'Aujourd'Hui*, 241, 12–20.
- [6] Winartomo B., Vroomen U., Buhrig-Polaczek A., Pelzer M. (2005). Multiphase modelling of core shooting process. *International Journal of Cast Metals Research*, 18(1), 13–20.
- [7] Wu J., Cui Y., Li W. (2002). Computer simulation of core-shooting process with two-phase flow. *International Journal of Cast Metals Research*, 15, 445–449.
- [8] Ni C.J., Lu G.C., Zhang Q.D., Jing T., Wu T.J., Yang L.L., Wu Q.F. (2016). Influence of core box vents distribution on flow dynamics of core shooting process based on experiment and numerical simulation. *China Foundry*, 13(1), 22–26.